

The proposal of a hysteretic model for internal wooden walls in Pombalino buildings

*Helena Meireles¹⁾, Rita Bento²⁾, Serena Cattari³⁾ and Sergio Lagomarsino⁴⁾

^{1),2)}ICIST, Instituto Superior Técnico, The Technical University of Lisbon, Portugal

^{3),4)}Department of Civil, Environmental and Architectural Engineering, University of Genoa,
Italy

¹⁾hmeireles@civil.ist.utl.pt

ABSTRACT

The heritage value of the mixed wood-masonry 18th century *Pombalino* buildings of downtown Lisbon is recognized both nationally and internationally. These buildings have a three-dimensional timber structure composed of wooden floors, stairs and walls intended to provide increased seismic resistance. The three-dimensional timber structure is enclosed in surrounding unreinforced masonry walls. The interior wooden walls are called “frontal” walls and their behavior under cyclic loading has hardly been studied. This paper describes the proposal of a hysteretic model for the cyclic behaviour of these *Pombalino* “frontal” walls. The hysteresis model, based on phenomenological approach, aims to reproduce the response of a wall under general monotonic, cyclic or earthquake loading and is based on a minimum number of path following rules. The model is constructed using a series of exponential and linear functions. There are total of nine identifiable parameters in this model to capture the nonlinear hysteretic response of the wall. These are all calibrated with experimental data. In particular, the analytical model proposed herein is calibrated based on the experimental testing performed previously by the same authors. The model developed also accounts for characteristics such as pinching effect, strength and stiffness degradation that have been observed in the experimental data.

1. INTRODUCTION

The heritage value of the mixed wood-masonry 18th century *Pombalino* buildings in downtown Lisbon is recognized both nationally and internationally. In 1755 a catastrophic earthquake followed by a major tsunami struck the capital of Portugal causing severe damage to the city. The event completely destroyed the heart of the city, which was set on a valley area close to the river Tejo and is composed of a shallow layer of alluvial material. The disaster required an urgent solution. The Prime Minister at the time, Marquis of *Pombal*, was put in charge of rebuilding the city and restoring it back to normality as fast as possible. He delegated to a group of engineers the development of a structural solution that would guarantee the required seismic resistance of the buildings. Based on the know-how of that time and on the empirical knowledge gathered from the buildings that survived the earthquake a new type of construction was created, which is now generally referred to as *Pombalino* construction. An example of the construction elements that compose a *Pombalino* building can be seen in Fig. 1.

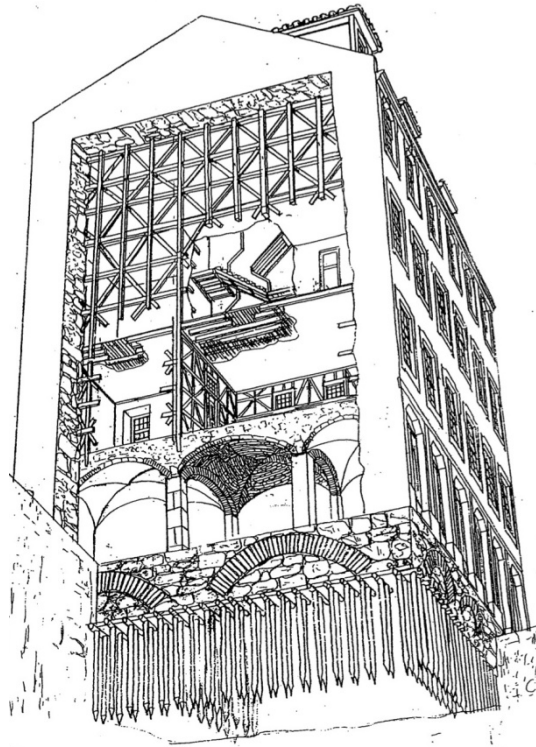


Fig 1. Example of a *Pombalino* building (Mascarenhas, 2005).

This construction type is summarized below, based on Mascarenhas (2005). The buildings were built in quarters comprising each quarter an average of 10 buildings. The foundation system was ingenious; it is based on a system of wooden piles over the alluvium layers. The piles are similar and repetitive, on average 15 cm in diameter and 1.5 m in length. These form two parallel rows in the direction of the main walls, which were linked at the top by horizontal wood cross-members attached by thick iron nails. The construction at ground floor consisted of solid walls and piers linked by a system of arches. In more elaborate cases, thick groined vaults spanned between the arches, which protected the upper floors from the spread of any fire that might start at ground floor level. From the first floor up the basis of this building system is a three-dimensional timber structure called “gaiola” (cage), thought to be an improved system based on prior traditional wooden houses. The “gaiola” is composed of traditional timber floors and improved mixed timber-masonry shear walls (“frontal” walls) that would support not only the vertical loads but also act as a restraint for the seismic horizontal loading. However, no analytical models with any structural software have proven that so far and we have to assume the current lack of knowledge in predicting the role of these “frontal” walls in the seismic resistance of the buildings. Nevertheless, these “frontal” walls are one of the main speciousness of these buildings. They consist of a wooden truss system filled with a weak mortar in the empty spaces.

Very few data, analytical and experimental, exists on the behaviour of the “frontal” walls. Such data can be obtained from experiments consisting of physical tests of representative specimen. For this reason it is important to carry out experimental work that can further back up analytical computer models. The work of Meireles and Bento (2010) was the first to test the

“frontal” walls under static cyclic shear testing with imposed displacements, where a specific loading protocol was used and vertical loading applied. The objective of the experimental work developed in the cited paper was, therefore, to obtain the hysteretic behavior of these “frontal” walls, by means of static cyclic shear testing with imposed displacements. These properties shall be used in developing an analytical hysteretic model of the structure, which is the scope of the present paper.

2. HYSTERESIS MODEL

2.1 Presentation of the model

An hysteresis model was developed based on a minimum number of path following rules that can reproduce the response of the wall tested under general monotonic or cyclic loading. The model was calibrated according to the experimental results obtained. The model is constructed using a series of exponential functions and linear functions. There are total of 9 identifiable parameters in this model to capture the nonlinear hysteretic response of the wall. Fig. 2. shows the assumed load-deformation behaviour of the wall.

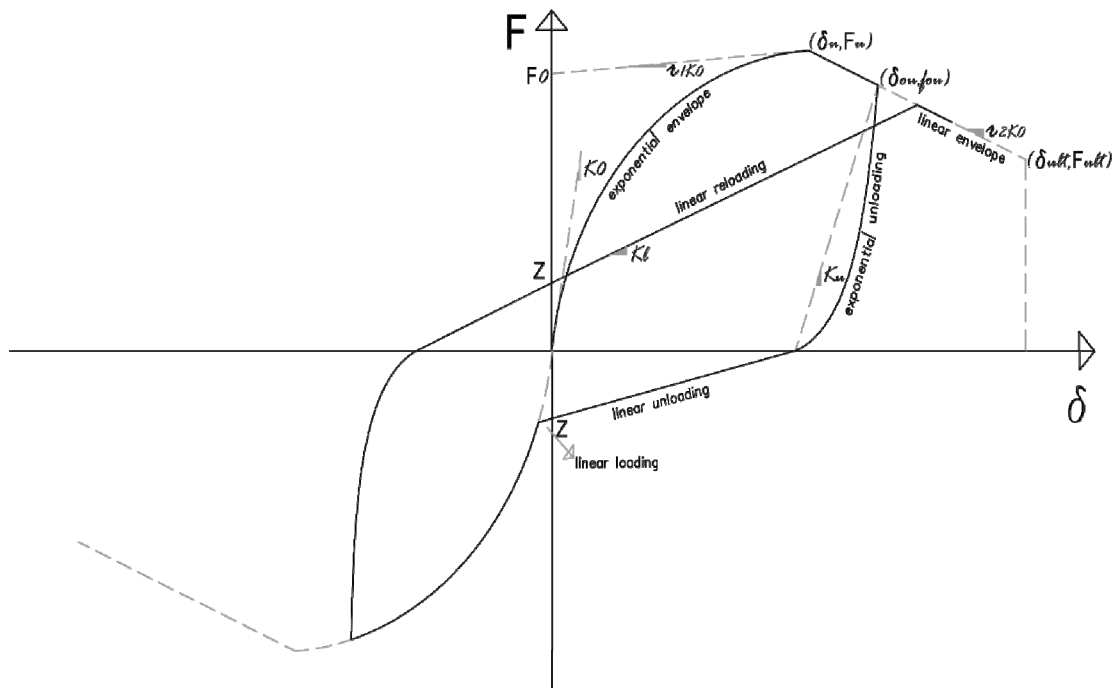


Fig. 2. Hysteresis model.

2.2 Path following rules

The first step for obtaining a hysteresis model is to define the envelope curve. It is assumed that the envelope curve is independent of the loading history and coincides approximately with the stress-strain curve obtained under monotonic loading. Once the envelope is determined the loading and unloading paths must be described. Loading (or reloading) paths are identified as cases where both the displacement δ , and the gradient, $\Delta\delta$, of the displacement have the same

signs ($\delta^*\Delta\delta>0$). In contrast, unloading paths correspond to cases where the displacement and the gradient of the displacement have opposite signs ($\delta^*\Delta\delta<0$).

The path following rules are such that the structure loaded in the first cycle will draw the envelope curve. It follows an unloading path at a certain point and the loading in the opposite direction. A *linear loading* branch is defined in the model so as to have a transition between the point Z (figure 2) and the envelope curve when the structure is loaded in the opposite direction for the first time. The meaning of Z point will be explained later. Afterwards, when the structure is loaded again in the initial direction, it will reload with a reloading path which is not the same as the envelope path. When the structure reloading path reaches the envelope curve it means the structure is being loaded for the first time for those displacements; it happens then that the envelope curve is followed again. Again, unloading can happen at any point.

In the following sections, the procedures for constructing the envelope, the loading/reloading and unloading curves within the model are discussed. For clarity of discussion the equations presented in the following sections are exclusively for positive displacement of the hysteretic loops. Implementation of these equations for the negative displacement region implies the reversal of the sign at certain variables and the use of absolute values in others.

2.3 Definition of the envelope curves

The monotonic pushover response of the wall is modelled using one exponential and one linear function. The exponential function defines the ascending branch (*exponential envelope*) and the linear function the descending branch (*linear envelope*), see figure 2. The envelope curve is defined by 6 identifiable parameters that must be fitted to experimental data. The parameters, illustrated in figure 2, are F_0 , K_0 , r_1 , r_2 , δ_u and δ_{ult} . The respective mathematical functions are the following:

$$F = \begin{cases} (F_0 + r_1 K_0 \delta) \cdot (1 - e^{(-K_0 / F_0 \delta)}) & \text{for } \delta \leq \delta_u & (a) \\ F_u + r_2 K_0 (\delta - \delta_u) & \text{for } \delta_u < \delta \leq \delta_{ult} & (b) \\ 0 & \text{for } \delta > \delta_{ult} & (c) \end{cases} \quad (1)$$

The exponential function used to describe the ascending branch (1)(a) was first proposed by Foschi (1974) and later used by Folz and Filiatrault (2001) in the modelling of wood shear walls response for the CUREE model. Beyond the displacement δ_u , which corresponds to the ultimate load F_u the load-carrying capacity is reduced. Failure of the wall under monotonic loading occurs at displacement δ_{ult} . It has been assumed the wall's monotonic deformation capacity δ_{ult} is defined as the deformation at which the applied load drops to **80%** of the maximum (ultimate) load F_u that was applied to the specimen. In this case, δ_{ult} is already defined based on r_2 , δ_u and F_u . So, the number of identifiable parameters is reduced to **5**.

2.4 Definition of the unloading curves

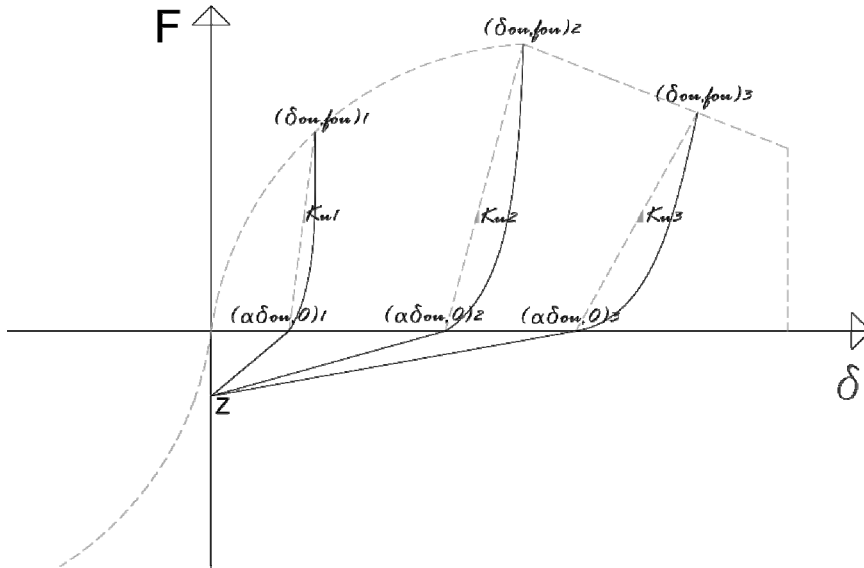


Fig. 3. Hysteresis model: unloading.

Observation of the hysteretic loops of the walls tested in the work of Meireles and Bento (2010) reveals a curved shape unloading branch until the zero force intercept and a relatively linear branch from that point until the zero displacement intercept. It also reveals a degrading unloading stiffness if we consider this stiffness to be K_u in figure 3 (K_{u1} to K_{u3}). This degradation is related to the point of the start of the unloading δ_{ou} ; the unloading stiffness K_u is decreasing with increasing values of δ_{ou} . An exponential function that is capable of capturing this fact has been defined. The mathematical formulation is the following:

$$\begin{cases} F = K_u (\delta - \alpha \delta_{ou}) e^{\lambda_u (\delta - \delta_{ou})} & (a) \\ K_u = \frac{f_{ou}}{\delta_{ou} (1 - \alpha)} & (b) \end{cases} \quad (2)$$

The variables δ_{ou} and f_{ou} are the initial unloading displacement and force, respectively. Equation (2) satisfies the boundary conditions $F(\delta = \delta_{ou}) = f_{ou}$ and $F(\delta = \alpha \delta_{ou}) = 0$. The unloading exponential curve requires the knowledge of 2 identifiable parameters α and λ_u , which define, respectively, the displacement intercept point and the shape of the exponential curve. These two parameters must be calibrated with experimental data. The parameter α is fixed for all the loops or for all values of δ_{ou} ; on the contrary, the parameter λ_u is not constant and will be a function of δ_{ou} as will be explained later. During the unloading process, the variables δ_{ou} and f_{ou} are known and thus are not parameters that need to be defined.

When the unloading starts at point (δ_{ou}, f_{ou}) it will reach the point $(\alpha \delta_{ou}, 0)$. After this a linear function (*linear unloading*) is defined from this point until the point $(0, Z)$ where the force intercept parameter is called Z . From the observation of the experimental data we can see that

the pinched hysteresis loops are very much close to passing through the same force intercept, although they do not exactly do so. For simplicity of the model it was assumed the same force intercept for all the loops. This parameter, Z , has to be calibrated with experimental data.

2.5 Definition of the reloading curves

One important characteristic that could be observed in the response of these walls is the degradation of the restoring force, commonly known as strength degradation. In this situation, it is observed that the reloading curve does not reach the point of maximum displacement (δ_{max} , F) at the envelope curve but instead is pointing to a point which is lower by a certain amount of force (for instance a). As a consequence of this the stiffness decreases also by a certain amount or it degrades (stiffness degradation). In the model defined, see figure 4, the strength degradation was estimated by calculating the force reduction parameter a for each level of damage. The damage is herein assumed to be related to the maximum drift attained so far and is a variable that is calculated at each loop based on all the history of the force-displacement response. In this way, a linear reloading curve is drawn from the point Z to the damaged point which stays below the point (δ_{max} , F). At the beginning of a reloading path the initial point at y -intercept, Z , is known. The force reduction parameter a is calibrated based on the experimental results and is not a fixed parameter varying with the accumulation of damage on the structure.

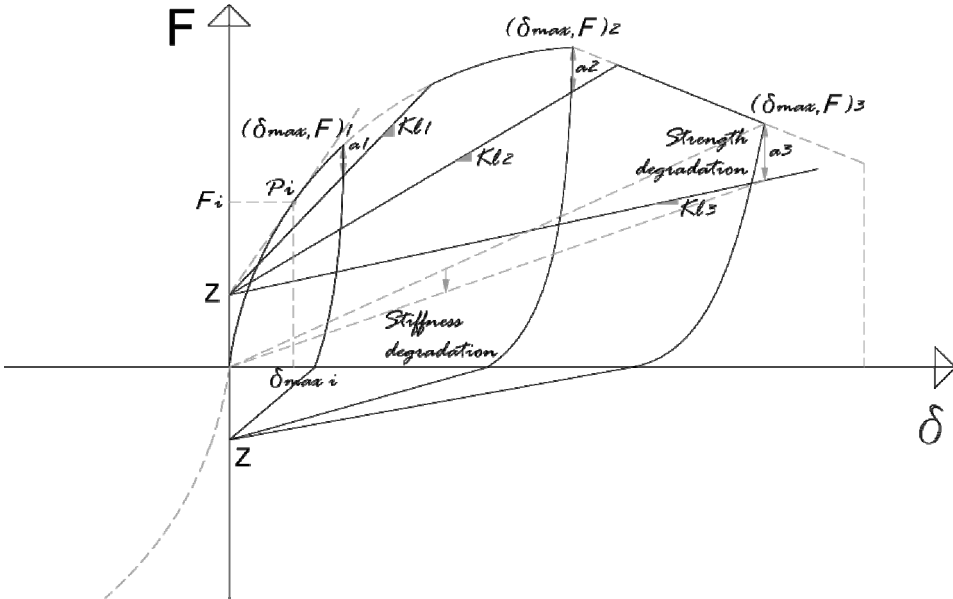


Fig. 4. Hysteresis model: reloading.

In this way, strength degradation is directly estimated but the stiffness degradation is indirectly accounted for in this modelling technique. In other models seen by the authors, as opposed, the strength degradation is indirectly accounted for.

An aspect related to this modelling is the fact that for all the lower or equal values of damage associated to displacement at point P_i (δ_{max}^i , F^i) the linear reloading curve will always point to

the point P_i and never to a lower value. It can be said that no damage is seen for this point or before that. Point P_i is calculated as the point belonging to the envelope curve and the linear function that starts at Z and is tangent to the envelope curve. This is to avoid that the linear reloading curve has a low derivative for small initial values of displacement, when there is no assumed damage, or even to avoid it from having negative derivatives for very small values of displacement (given that the linear reloading curve starts at Z and not at origin). As a consequence, the reloading gradient Kl is constant until the point P_i and then decreases with increasing damage, see Fig. 13. The formula for determining δ_{max}^i (and thus the point P_i) and rl at point P_i is the following:

$$\begin{cases} F'(\delta_{max}^i) = E'(\delta_{max}^i) \\ F(\delta_{max}^i) = E(\delta_{max}^i) \end{cases} \Leftrightarrow \begin{cases} rl K_0 = r_1 K_0 \cdot \left(1 - e^{-K_0 \delta_{max}^i / F_0}\right) + (F_0 + r_1 K_0 \delta_{max}^i) \cdot K_0 / F_0 \cdot e^{-K_0 \delta_{max}^i / F_0} \\ rl K_0 \delta_{max}^i + Z = (F_0 + r_1 K_0 \delta_{max}^i) \cdot \left(1 - e^{-K_0 \delta_{max}^i / F_0}\right) \end{cases}$$

$$\Leftrightarrow \begin{cases} rl = \dots \\ \delta_{max}^i = \dots \end{cases}$$

Where $F(\delta)$ and $E(\delta)$ are, respectively, the linear curve that goes from Z to P_i and the exponential envelope curve.

□

2.6 Small cycle hysteresis

The rules previously described define complete loops, which are loops that undergo complete unloading. In order to have a more general model, one that could be subjected to any type of loading, and not restricted to cyclic loading, we need to account also for situations where reloading can happen at any place during the loading/unloading history. This leads to small cycle or incomplete cycle hysteresis. Crisafulli (1997) focused on the issue of incomplete cycle hysteresis when related to concrete elements and conducted tests on standard concrete cylinders with different combinations of complete and incomplete loops. The most important conclusions drawn herein were that the successive inner loops do not affect the plastic deformation and remain inside the cycle defined for the complete unloading and reloading curves. This is shown in the figure 5 below:

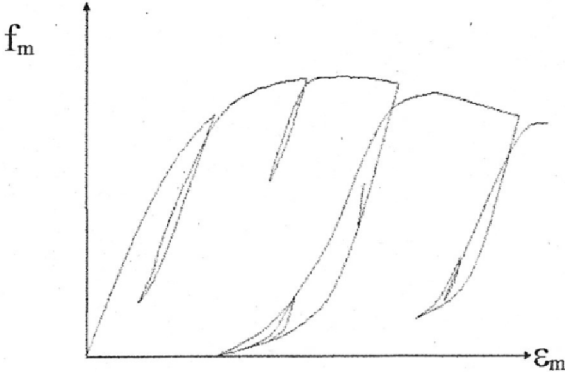


Fig. 5. Typical cyclic response with small cycle hysteresis for concrete (Crisafulli, 1997)

In the proposed model herein, because of the lack of any other information or data, it was simply assumed that the structure would reload with a linear branch (*linear reloading small cycle*) until it would reach the previously defined *linear reloading* branch. This would happen both if the reloading would take place at the *exponential unloading* branch or at the *linear unloading* branch. The new linear branch defined has the derivative K_0 , equal to the initial stiffness. The following figure 6 shows these assumptions.

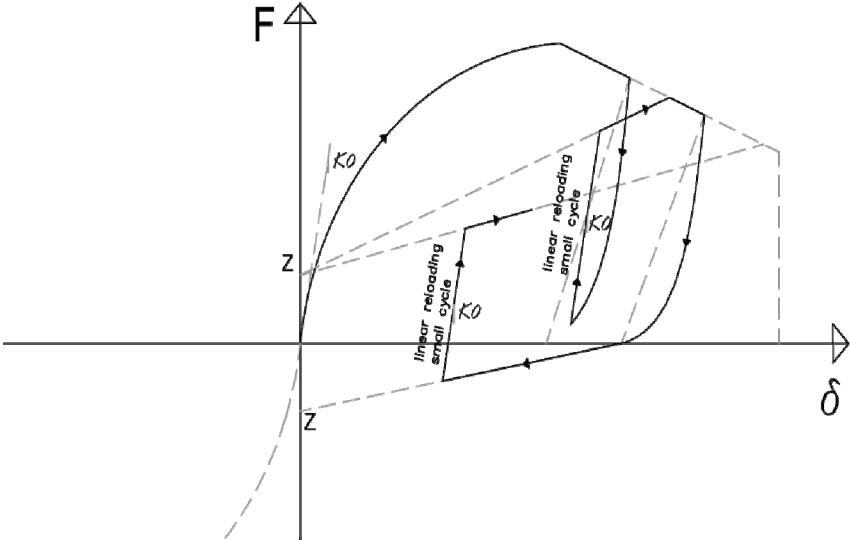


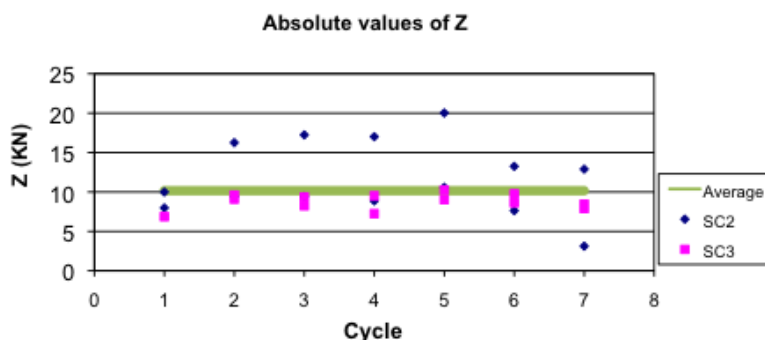
Fig. 6. Model assumptions for the small cycle hysteresis.

3. CALIBRATION OF THE PARAMETERS

The parameters associated to the hysteresis model must be fitted to experimental data. This can be accomplished by least-square regression of the functions or by the averaging of point parameters.

3.1 Force intercept parameter – Z

The force intercept parameter is called Z . For simplicity of the model it was assumed the same force intercept for all the loops, which is not far away from reality. Based on the experimental data we can plot all the force intercepts, be they positive or negative, and obtain the average



point Z . In Fig. 7. it can be seen all the force intercepts and the average value obtained for Z ($Z=10.16$).

Fig. 7. Average force intercept point Z .

3.2 Envelope curve parameters - F_0 , K_0 , r_1 , r_2 , F_u , δ_{ult}

The values obtained for the envelope curve parameters can be seen in table 1.

Table 1 Envelope curve parameters.

F_0 (KN)	37.00
r_1	0.04
K_0 (KN/mm)	6.1
r_2	-0.045
F_u (KN)	50.83
δ_{ult} (mm)	93.71 (3.8% drift)

As explained before, failure of the wall under monotonic loading occurs at displacement δ_{ult} . It has been assumed the wall's monotonic deformation capacity, δ_{ult} , is defined as the deformation at which the applied load drops to **80%** of the maximum (ultimate) load F_u that was applied to the specimen. In this way, δ_{ult} is already defined based on r_2 , δ_u and F_u . This corresponds to a ultimate drift of 3.8%. Accordingly, the couple values of (F_u, δ_u) and (F_{ult}, δ_{ult}) are the following depicted in table 2.

Table 2 Couple values of (F_u, δ_u) and (F_{ult}, δ_{ult})

δ_u (mm)	56.68	δ_{ult} (mm)	93.71
F_u (KN)	50.83	F_{ult} (KN)	40.67

The value of K_0 has been taken from the experimental initial stiffness at a displacement of 3 mm. The average value as been assumed based on the SC2 and SC3 test results (Meireles and Bento, 2010). The values of F_0 and r_1 have been determined by least-square regression of the function *envelope exponential*. The following figure 8 shows the *exponential envelope* curve for the calibrated parameters and the corresponding experimental points for both negative and positive

loading. Herein, it can be seen how well the obtained analytical *exponential envelope* curve fits the experimental envelope points.

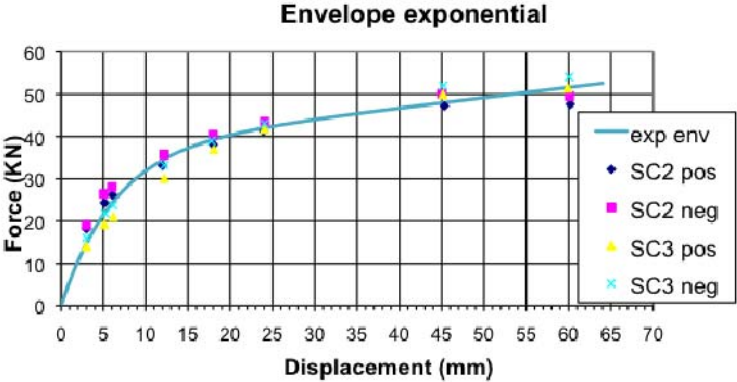


Fig. 8. Exponential envelope curve.

The value of r_2 has been calculated by least-square regression of the function *envelope linear*. Figure 9 shows the *linear envelope* curve for the calibrated parameter, r_2 , and the corresponding experimental points for both negative and positive loading. Herein, it can be seen how well the analytical linear envelope curve fits the experimental envelope points.

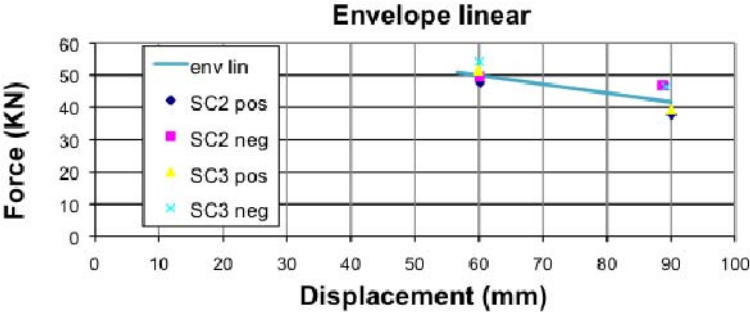


Fig. 9. Linear envelope curve.

3.3 Unloading curve parameters - α, λ_u

The value of α is taken as the average of all the obtained experimental values of α for positive or negative displacements. The value of α is estimated as 0.55. The plot of figure 10 shows the values of α as a function of the experimental unloading points δ_{ou} (dou in the plot). Herein, it can be seen how well the value of α fits the experimentally obtained points.

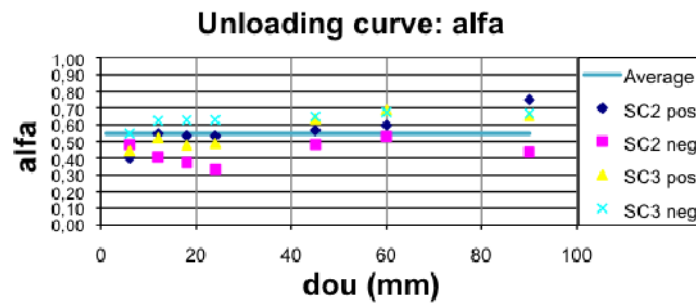


Fig. 10. Unloading curve parameter α .

The value of λ_u is the one defining the shape of the unloading exponential curve, as has been seen before. The plot of the values of λ_u as a function of the unloading point δ_{ou} (dou in the plot) is shown in the figure 11. Based on these results, it has been decided that the parameter λ_u cannot be a constant value but is better approximated by a logarithmic function dependent of δ_{ou} (dou in the plot). The equation for λ_u as a function of δ_{ou} (dou in the plot) is given by:

$$\lambda_u = -0.087 \cdot \ln(\delta_{ou}) + 0.4593 \quad (3)$$

The figure 11 is found below:

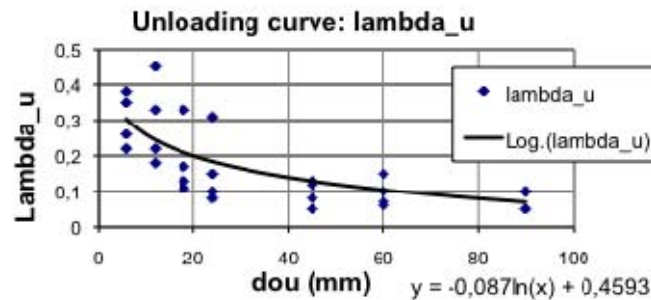


Fig. 11. Unloading curve parameter λ_u .

3.4 Reloading curve parameter – a

In the model defined, the strength degradation was estimated by calculating the force reduction parameter a for each level of damage. Figure 12 depicts the experimentally obtained values of a as a function of the maximum drift obtained so far. Herein the damage of the wall is associated to the interstorey drift of the wall. Inter-story drift is a key parameter for the control of damage in wood framed buildings (Filiatrault, 2002). In figure 12, the linear approximation by least-square regression is also presented for the parameter a . The equation of a as a function of the damage (maximum drift) of the wall is obtained as:

$$a = 5.0585 \cdot \text{Drift} - 0.0004 \quad (4)$$

Figure 12 is presented as follows.

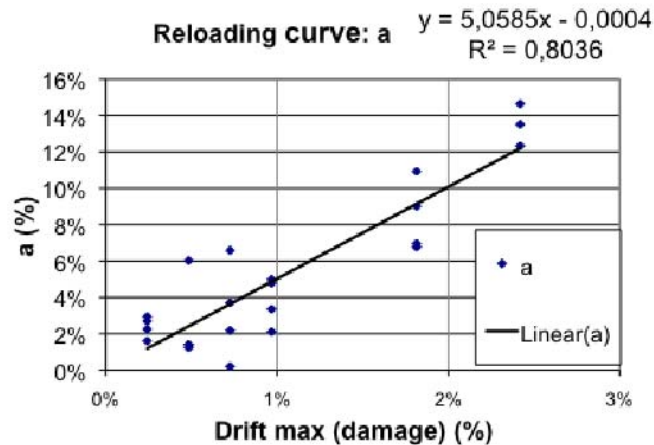


Fig. 12. Parameter a as a function of the damage.

As a consequence of the previous, we can calculate the reloading stiffness Kl (or the corresponding coefficient $rl=Kl/K0$). As has been explained previously, the reloading stiffness Kl (or the corresponding coefficient rl) are constant until the point Pi . In the following plot of Fig.13. it is presented the reloading curve coefficient, rl , as a function of the damage (or the maximum drift). Herein rl at point Pi equals 0.375 (and the displacement, δ^i , at point Pi equals 6.5 mm). The values of rl end for the maximum drift established of 3.8% associated to the collapse of the wall.

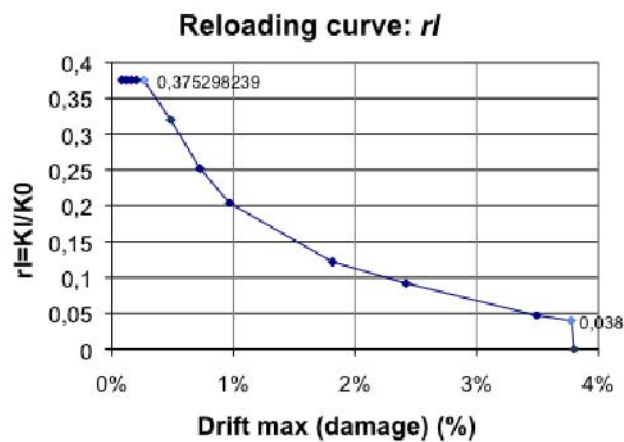


Fig. 13. Reloading curve coefficient rl as a function of damage.

4. EXPERIMENTAL VERSUS ANALYTICAL HYSTERESIS

A plot has been drawn for comparison of the hysteresis curves obtained experimentally and the hysteresis curve developed analytically. A good matching is obtained as can be seen in figure 14.

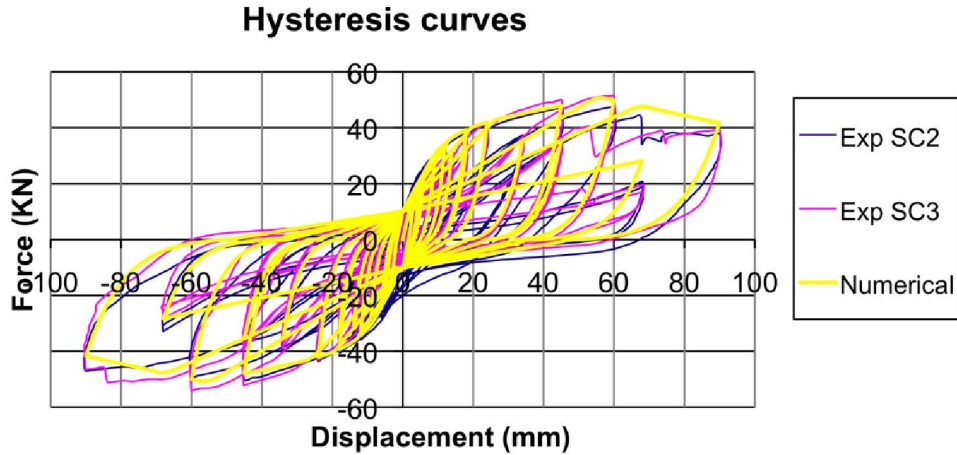


Fig. 14. Experimental versus analytical hysteresis.

The accuracy of the model response is determined using one error indicator which is the cumulative energy error (CEE). The CEE is defined as:

$$CEE = \frac{|CE_{test} - CE_{anal}|}{|CE_{test}|}$$

Where CE_{test} and CE_{anal} are the cumulative energy dissipation of the hysteresis of the experimental testing and of the analytical model, respectively. The cumulative energy dissipated by the wall, CE , is calculated as:

$$CE = \sum_i \int_{\delta_{i-1}}^{\delta_i} F(\delta) d\delta \approx \sum_i \frac{F_i + F_{i-1}}{2} (\delta_i - \delta_{i-1})$$

Where the subscript i is the i^{th} force-displacement ($F-\delta$) data point. The total percent error in cumulative energy dissipated between the fitted model and the actual cyclic test data is 9% for the test SC2 and 14% for the test SC3, indicating a good match between the analytical model and the experimental results.

CONCLUSIONS AND FURTHER WORK

A new hysteretic model for wood “frontal” walls has been developed. This is the first hysteretic model developed in the literature for such walls and thus its relevancy. The hysteretic model is governed by path following rules and is composed of linear and exponential functions. It is governed by 9 identifiable parameters. These parameters have been calibrated with experimental test results. The total percent error in cumulative energy dissipated between the fitted model and the actual cyclic test data is 9% for the test SC2 and 14% for the test SC3, accounting the good performance of the model. The model developed also accounts for characteristics such as pinching effect, strength and stiffness degradation that have been observed in the experimental data.

The results obtained herein are essential for further work in modelling the behaviour of such walls under monotonic, cyclic or earthquake loading. They are also necessary for the further work of the authors in developing a *macro-element* for “frontal” walls. This is to be implemented in a structural software, called 3Muri (www.stadata.com), which relates to the analysis of masonry buildings based on a macro-element approach (Lagomarsino and Cattari, 2009). Also it will be predicted the hysteresis curve for other wall sizes (height and length), since in reality we can find different wall sizes in a single building. Further ahead the authors will model a complete building in 3Muri and make use of the developed macro-element to include the “frontal” walls.

ACKNOWLEDGEMENTS

It is acknowledged the financial support of the Foundation for Science and Technology (FCT) in terms of a doctorate scholarship awarded to the main author, reference SFRH/BD/41710/2007.

REFERENCES

- Crisafulli FJ, (1997) Seismic behaviour of reinforced concrete structures with masonry infills, Ph.D. Thesis, Department of Civil Engineering, University Canterbury, New Zeland.
- Filiatrault A, Isoda H, Folz B, (2002), Hysteretic damping of wood framed buildings, *Engineering Structures* 25, 416-471.
- Foschi RO, (1974), Load-slip characteristics of nails, *Wood Sci.*, 7(1), 69-76.
- Folz B, Filiatrault A, (2001), Cyclic analysis of wood shear walls, *Journal of Structural Engineering ASCE*, 433-441
- Lagomarsino S., Cattari S. (2009). Non linear seismic analysis of masonry buildings by the equivalent frame model. Proc. 11^o D-A-CH Conference: Masonry and earthquakes (invited paper), Zurich, 10-11 September 2009, pp. 85-100. ISBN 978-3-03732-021-1.
- Mascarenhas J., (2005), *Sistemas de Construção V-O Edifício de rendimento da Baixa Pombalina de Lisboa, Materiais Básicos 3^o Parte: O Vidro. Livros Horizonte* (in Portuguese).
- Meireles H., Bento R., (2010), Cyclic behaviour of Pombalino “frontal” walls, 14th European Conference on Earthquake Engineering, pp.325, Ohrid, Macedonia.
- 3Muri Program release 3.2.11 <http://www.stadata.com> (solver algorithm developed by Lagomarsino S., Galasco A., Penna A., Cattari S.)